

Improved Slice-wise Tumour Detection in Brain MRIs by Computing Dissimilarities between Latent Representations

Alexandra-Ioana Albu
Romanian Institute of Science and
Technology
Babeş-Bolyai University
Cluj-Napoca, Romania
albu@rist.ro

Alina Enescu
Romanian Institute of Science and
Technology
Babeş-Bolyai University
Cluj-Napoca, Romania
enescu@rist.ro

Luigi Malagò
Romanian Institute of Science and
Technology
Cluj-Napoca, Romania
malago@rist.ro

ABSTRACT

Anomaly detection for Magnetic Resonance Images (MRIs) can be solved with unsupervised methods by learning the distribution of healthy images and identifying anomalies as outliers. In presence of an additional dataset of unlabelled data containing also anomalies, the task can be framed as a semi-supervised task with negative and unlabelled sample points. Recently, in Albu et al., 2020, we have proposed a slice-wise semi-supervised method for tumour detection based on the computation of a dissimilarity function in the latent space of a Variational AutoEncoder, trained on unlabelled data. The dissimilarity is computed between the encoding of the image and the encoding of its reconstruction obtained through a different autoencoder trained only on healthy images. In this paper we present novel and improved results for our method, obtained by training the Variational AutoEncoders on a subset of the HCP and BRATS-2018 datasets and testing on the remaining individuals. We show that by training the models on higher resolution images and by improving the quality of the reconstructions, we obtain results which are comparable with different baselines, which employ a single VAE trained on healthy individuals. As expected, the performance of our method increases with the size of the threshold used to determine the presence of an anomaly.

CCS CONCEPTS

• **Computing methodologies** → **Anomaly detection**; *Latent variable models*; Reconstruction.

KEYWORDS

Anomaly Detection, Brain Magnetic Resonance Imaging, Variational AutoEncoders

ACM Reference Format:

Alexandra-Ioana Albu, Alina Enescu, and Luigi Malagò. 2020. Improved Slice-wise Tumour Detection in Brain MRIs by Computing Dissimilarities between Latent Representations. In *2020 KDD Workshop on Applied Data Science for Healthcare*, August 24, 2020, San Diego, CA, USA. ACM, New York, NY, USA, 4 pages.

Permission to make digital or hard copies of all or part of this work for personal or classroom use is granted without fee provided that copies are not made or distributed for profit or commercial advantage and that copies bear this notice and the full citation on the first page. Copyrights for components of this work owned by others than the author(s) must be honored. Abstracting with credit is permitted. To copy otherwise, or republish, to post on servers or to redistribute to lists, requires prior specific permission and/or a fee. Request permissions from permissions@acm.org.

DSHealth'20, August 24, 2020, San Diego, CA, USA

© 2020 Copyright held by the owner/author(s). Publication rights licensed to ACM.

1 INTRODUCTION

Automatic outlining of anomalies in brain Magnetic Resonance Images (MRIs) is of great importance in computer-aided diagnosis, in order to develop reliable systems that can assist physicians in diagnosing pathologies. Indeed, accurate diagnosis is not only time consuming, but also requires a lot of experience and high sensitivity to the specific condition. The study conducted by Drew et al. [6] showed that diagnoses are vulnerable to perceptual blindness, and this can lead to high miss rates of anomalies.

Deep learning has been employed extensively in medical imaging, with a track of very good results in the last years, see [10] for a review. However, one of the limitations to the use of deep neural networks is given by the need of large datasets, which may be difficult to be obtained, especially if they need to be annotated. In the last years, this has lead to an increased interest for the design of unsupervised and semi-supervised methods. In the context of anomaly detection for medical images, a common approach consists in learning a distribution for the hidden representations of images of healthy individuals in a completely unsupervised way, and then identifying anomalies as those encodings which behave as outliers. On the other side, there are settings as for brain tumour detection from MRIs in which datasets of unhealthy individuals are available, and they could be exploited as unlabelled data in learning for the design of semi-supervised methods in presence of negative and unlabelled samples.

In our previous work [1], we have designed a slice-wise tumour detection algorithm based on Variational AutoEncoders (VAEs) for tumour detection in brain MRIs from two publicly available datasets, HCP [16] and BRATS-2015 [9, 11]. Our algorithm is based on the computation of a distance, or more generically a dissimilarity function, in the space of the approximate posteriors of a VAE, trained on both healthy (or normal) and tumoural tissues. The method requires to train an additional VAE only on healthy images, used to reconstruct unlabelled slices. The classifier is based on the computation of the distance between the encoding of an original image and the encoding of its reconstruction. The algorithm is semi-supervised with negative and unlabelled data.

Preliminary experiments from [1] showed that the performance of our method in detecting slices which contain tumours directly depends on the quality of the reconstructions obtained with the two VAEs and in particular on the capability of the first VAE, trained only on healthy images, to remove the tumoural tissues in the reconstructed image. In this paper we present novel and improved

results in which we evaluate our algorithm on the HCP and BRATS-2018 datasets, using higher resolution images and models able to produce better reconstructions.

VAEs are powerful generative models with probabilistic latent variables which have been successfully employed in various segmentation or anomaly detection tasks in medical applications [3, 12, 14, 18]. Generative models are particularly well suited for anomaly detection, as they can be used to learn the distribution of healthy tissues and then identify anomalies as out-of-distribution behaviours.

Unsupervised or semi-supervised anomaly detection methods typically use various types of autoencoders trained on healthy data, relying on the fact that anomalies, which were not seen during training, cannot be properly reconstructed. The encoder-decoder architecture is particularly useful as the anomaly segmentation can be easily obtained as a pixel-wise difference between the original image and its reconstruction [3–5]. Chen et al. [4, 5] evaluated two generative models, VAEs and Adversarial AutoEncoders, for the task of detection of tumours and stroke lesions in brain MRIs. Additionally, [4] proposes the use of a regularizer that encourages the models to learn more suitable latent space representations for healthy and unhealthy images. In [19] Zimmerer et al. highlighted the limitations of using a plain reconstruction error for detecting anomalous pixels and proposed instead to quantify the abnormality of input pixels using the derivative of the log-likelihood with respect to the inputs. In [18] a context-encoding regularizer was added to the VAEs loss function, obtaining a Context Encoding VAE (ceVAE) which has shown significant improvements compared to previously proposed methods. Another approach combining the benefits of an autoencoder architecture and adversarial training, the Adversarial Dual Autoencoder (ADAe), was proposed in [17].

The paper is organized as follows. In Section 2 we review our algorithm for anomaly detection based on the computation of dissimilarities between latent representations of a Variational AutoEncoder. In Section 3 we present our experimental setting, while Section 4 shows that our method can discriminate between images containing tumours and healthy scans, and compares favourably with different baselines which employ a single VAE trained on healthy individuals. Finally, Section 5 outlines the conclusions and future works.

2 ANOMALY DETECTION ALGORITHM

In this section we briefly present our algorithm for slice-wise anomaly detection in brain MRIs based on Variational AutoEncoders (VAEs), firstly introduced in [1]. The algorithm is based on the use of VAEs [8, 13], i.e., generative models which consist of two neural networks: an encoder and a decoder. The encoder maps the input to the parameters θ of a probability density function q_θ over the latent space, while the decoder maps the latent representation to a probability density function p_ϕ over the space of the observations. VAEs are trained by maximizing a lower bound for the log-likelihood, which consists of a reconstruction error and a Kullback-Leibler penalty term. For each input x , a VAE computes an approximate posterior from which the latent variables are sampled.

Our algorithm requires to train two VAEs on two different datasets, one containing only healthy subjects, VAE-H, and one containing brain scans that may or may not contain tumoural tissue, VAE. The proposed method is presented in Algorithm 1. Differently from our

previous approach, in order to obtain sharper reconstructions for high resolution images, we trained the VAE models by maximizing the likelihood only for pixels inside the brain mask. By using this technique, the model is able to focus on reconstructing finer brain structures details, however, background pixels can take arbitrary values. In order to obtain the original black background, the brain mask was overlapped on the reconstructed image.

To test the anomaly detection, we reconstruct a given image through the first model, VAE-H and compute the distance between the encodings through the second model VAE of the given image and its reconstruction. Due to the fact that the first model is trained only on normal tissues, it will not be able to reconstruct accurately anomalies, thus the distance between the two encodings will be larger for images containing abnormal regions.

Algorithm 1: Classification of brain MRIs from [1]

Input: Let d be a distance defined over the latent space of a VAE

Data: MRI-H: dataset of MRI slices of healthy individuals

Data: MRI: dataset of MRI slices of individuals which may have tumoural tissues

- 1 Let VAE-H be a VAE trained on MRI-H
 - 2 Let VAE be a VAE trained on MRI
 - 3 Let $x_h = \text{VAE-H.rec}(x)$ be the reconstruction of x through VAE-H
 - 4 Let $\text{VAE.enc}(x)$ be the encoding of x through VAE
 - 5 Let $d_x = d(\text{VAE.enc}(x), \text{VAE.enc}(x_h))$
 - 6 Compute the distribution of the distances d_x , with x in the validation set of MRI-H and let d_* be a threshold selected based on a percentile
 - 7 Compute d_x , with x in the test set of MRI, and classify the slice as healthy if $d_x < d_*$
-

3 EXPERIMENTAL SETTING

This section presents an overview the two datasets used in our experiments, alongside the methods used for preprocessing the data. Afterwards, the architectures of the networks and aspects related to the training procedure are outlined.

3.1 Datasets

Compared to our previous experiments [1], we used the same dataset of healthy individuals, i.e., the HCP dataset [16], but we evaluated our method on a newer version of the BRATS dataset, BRATS-2018 [9, 11]. We used a subset of the HCP dataset which contains 214 T2-weighted MRI scans of unrelated subjects. We removed the black slices keeping only 190 slices containing brain tissue from the HCP dataset, and we kept the middle 130 slices from the BRATS dataset. Both datasets were split into training, validation and test datasets, each representing 70%, 15% and 15% of the total amount of data.

The images have been preprocessed by applying bias field correction using the N4ITK algorithm [15], a variant of the popular nonparametric nonuniform intensity normalization (N3) algorithm, implemented in ANTSs [2]. Next, the 3D scans of both datasets have been normalized each in the $[-1, +1]$ range, and subsequently the histogram of each individual has been matched to a reference histogram associated to an image from the BRATS dataset. We have chosen to normalize with respect to an image coming from the

BRATS dataset since images have a larger variability compared to the HCP dataset due to the presence of tumoural tissues.

The images from both datasets have been cropped and resized to 200×200 and then down-sampled to 128×128 pixels. Furthermore, to avoid overfitting, the left and right hemispheres have been flipped with probability 0.5 during training and adjustment of brightness was applied, with delta 0.1 and probability 0.3. We further applied Gaussian white noise to the images given in input to the network.

3.2 Network Architectures

We have trained two VAEs with the same network topology. The encoders are represented by a sequence of convolutions with channels [64, 128, 256, 512], kernel size 4×4 and strides 2, followed by a stochastic layer of independent Gaussian distributions of dimension 128. The decoders are built symmetrically, with output channels [512, 256, 128, 64], kernel size 4×4 and strides 2. Similarly to our previous work, the output model is represented by a logit-normal distribution, for which we used a clip value for the mean equal to 0.01 for HCP and 0.001 for BRATS, a scalar covariance for HCP and vectorial for BRATS, with a minimum value of 0.01. When training the VAEs, the expectation is computed by generating 3 samples in the latent space for each input. The models have been trained using the Adam optimizer for 100 epochs, with a learning rate of 0.0001 and batch size of 32.

4 RESULTS

In this section we present novel and improved results, obtained by evaluating our anomaly detection algorithm on higher resolution images, using more powerful models able to provide better reconstructions.

As in [1], we have chosen in Algorithm 1 the distance function d to be the norm of the difference between the means obtained with VAE for the encodings of x and x_h . The threshold d_* used to classify images from the test set of BRATS has been computed as a percentile of the distances computed on the validation set of HCP. Differently from our previous work, where we fixed the 99% percentile, here we selected the percentile which maximizes the F1 score on the validation set of BRATS. In addition, we performed a 5-fold cross-validation scheme on the validation and test sets, by using 1/5 of the data to select the percentile and computing the performance metrics on the other 4/5 of the data.

We have used as anomaly scores for the computation of the ROC-AUC the distances in the latent space of VAE between the encoding of the original image and the encoding of its reconstruction through VAE-H. To validate our results, we have compared our method with different baselines using only the VAE trained on healthy images. These baselines are given by computing the L^2 norm of the difference between the original image and its reconstruction using VAE-H for different models.

Due to the resizing of the images, the area of a lesion is being reduced and thus small tumours may be difficult to be detected. To assess the impact of the tumour size on the performance, we evaluated our method for various numbers of anomalous pixels above which we consider slices to be unhealthy.

Our results, averaged over 5 splits and the corresponding standard deviations are presented in Table 1 for both our method and

several L^2 baselines trained only on healthy images. We considered a plain VAE, a denoising VAE with randomly placed grayscale square masks of size 40 in input (CE DVAE), and a VAE regularized by the L^2 distance between clean images and their reconstructions in presence of randomly placed grayscale square masks of size 20 (VAE + CE reg.), cf. [18]. The size of the masks are those which provided the best performance. Different thresholds for the tumour size have been considered. We can see that our method outperforms the baselines considering all metrics and tumour sizes. As expected, the performance increases with the threshold used to determine the presence of an anomaly.

We further depict in Table 2 a comparison of our approach with state-of-the-art unsupervised anomaly detection methods. Notice that a direct comparison is not possible, because of the different number of slices in the test set and the different version of the BRATS dataset. Compared to the two related approaches, we used a higher resolution for the images and a smaller test set, since we used part of BRATS dataset in training. We report the results for a tumour size threshold of 20, as in [18]. To evaluate the capability of our VAE-H model to remove the tumours from the BRATS images, we report some examples in Figure 1.

Table 1: Area Under the ROC Curve, accuracy and F1 score for BRATS-2018 (test set, averaged over 5 folds) for L^2 distances computed in the input space for different VAEs versus L^2 of the means in the latent space (our method [1]). $Th.$ denotes the threshold expressed in annotated pixels (before rescaling) used to determine if a slice contains anomalies.

Th.	Method	ROC-AUC	Accuracy	F1 score
0	L^2 input VAE	0.848 \pm 0.004	0.652 \pm 0.008	0.507 \pm 0.006
	L^2 input CE DVAE	0.864 \pm 0.004	0.656 \pm 0.008	0.505 \pm 0.007
	L^2 input VAE + CE reg.	0.865 \pm 0.003	0.736 \pm 0.003	0.679 \pm 0.004
	Our method	0.884 \pm 0.003	0.805 \pm 0.002	0.803 \pm 0.004
20	L^2 input VAE	0.851 \pm 0.004	0.673 \pm 0.007	0.520 \pm 0.005
	L^2 input CE DVAE	0.868 \pm 0.004	0.678 \pm 0.007	0.521 \pm 0.007
	L^2 input VAE + CE reg.	0.869 \pm 0.003	0.753 \pm 0.003	0.691 \pm 0.004
	Our method	0.890 \pm 0.004	0.809 \pm 0.002	0.803 \pm 0.005
50	L^2 input VAE	0.852 \pm 0.004	0.684 \pm 0.006	0.526 \pm 0.005
	L^2 input CE DVAE	0.871 \pm 0.004	0.691 \pm 0.006	0.531 \pm 0.007
	L^2 input VAE + CE reg.	0.873 \pm 0.003	0.762 \pm 0.002	0.698 \pm 0.004
	Our method	0.892 \pm 0.003	0.811 \pm 0.002	0.802 \pm 0.004
150	L^2 input VAE	0.856 \pm 0.004	0.707 \pm 0.005	0.541 \pm 0.005
	L^2 input CE DVAE	0.876 \pm 0.004	0.717 \pm 0.006	0.550 \pm 0.007
	L^2 input VAE + CE reg.	0.879 \pm 0.002	0.781 \pm 0.002	0.711 \pm 0.004
	Our method	0.897 \pm 0.004	0.814 \pm 0.002	0.795 \pm 0.005

Table 2: ROC-AUC for state-of-the-art and for our method. $Res.$ denotes the resolution of images after rescaling, and $Th.$ the threshold expressed in annotated pixels (before rescaling) used to determine if a slice contains anomalies.

Method	ROC-AUC	Dataset	# patients test set	Res.	Th.
ADAE [17]	0.892	BRATS2017	285	32x32	?
ceVAE [18]	0.867	BRATS2017	266	64x64	20
Our method [1]	0.890 \pm 0.004	BRATS2018	69	128x128	20

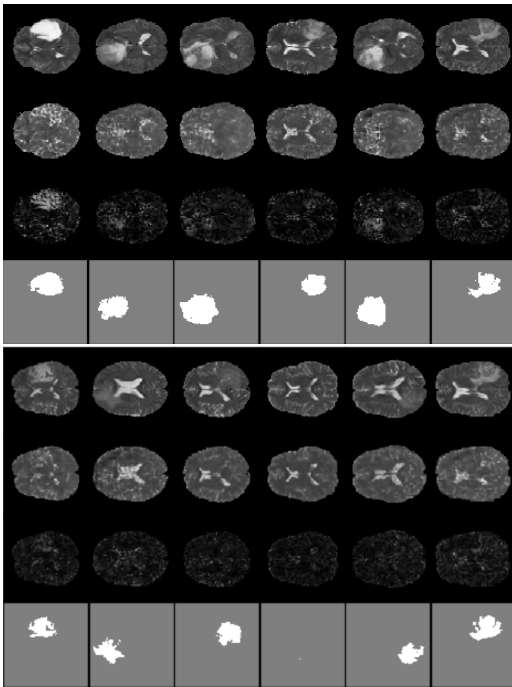


Figure 1: First row: original BRATS images from the test set. Second row: reconstruction through VAE-H of the original images. Third row: residual between original and reconstructed images. Fourth row: mask of the tumour. The two panels include cherry-picked slices to see the quality of the reconstructions and the associated residual images in different conditions.

5 CONCLUSIONS

In this paper, we have presented novel and improved results on anomaly detection for brain MRIs based on two Variational AutoEncoders (VAEs). Compared to our previous results [1], several changes have been made that have conducted to an improvement of the performance. A newer version of the BRATS dataset (BRATS-2018) has been used in training, together with a larger subset of the HCP dataset containing 214 individuals. Two additional steps in pre-processing have been introduced for both datasets: bias field correction using the N4ITK algorithm and matching of the histogram for each individual, using a reference histogram associated to an image from the BRATS dataset. In order to obtain sharper reconstructions, we trained the VAE models by maximizing the likelihood only for the pixels in the brain segmentation masks, which we have pre-computed. Additionally the choice of the best threshold has been obtained using a cross validation procedure, by removing the need to fix this parameter a priori.

We are currently investigating the possibility of improving the anomaly detection performance by using a perceptual loss which has been proved to increase the quality of the reconstructions [7] in other medical imaging datasets.

ACKNOWLEDGMENTS

The authors are supported by the DeepRiemann project, co-funded by the European Regional Development Fund and the Romanian Government through the Competitiveness Operational Programme 2014-2020, project ID P_37_714, contract no. 136/27.09.2016, SMIS code 103321. Data used in the preparation of this work were obtained from the Human Connectome Project (HCP) database¹ and the Multimodal Brain Tumor Segmentation Challenge (BRATS)².

REFERENCES

- [1] Alexandra Albu, Alina Enescu, and Luigi Malagò. 2020. Tumor Detection in Brain MRIs by Computing Dissimilarities in the Latent Space of a Variational AutoEncoder. In *Proc. of the Northern Lights Deep Learning Workshop*, Vol. 1. 6–6.
- [2] Brian B Avants, Nick Tustison, and Gang Song. 2009. Advanced normalization tools (ANTS). *Insight j* 2 (2009), 1–35.
- [3] Christoph Baur, Benedikt Wiestler, Shadi Albarqouni, and Nassir Navab. 2018. Deep autoencoding models for unsupervised anomaly segmentation in brain mr images. In *International MICCAI Brainlesion Workshop*. Springer, 161–169.
- [4] Xiaoran Chen and Ender Konukoglu. 2018. Unsupervised Detection of Lesions in Brain MRI using constrained adversarial auto-encoders. *Medical Imaging for Deep Learning (MIDL 2018)* (2018).
- [5] Xiaoran Chen, Nick Pawlowski, Martin Rajchl, Ben Glocker, and Ender Konukoglu. 2018. Deep generative models in the real-world: an open challenge from medical imaging. *arXiv:1806.05452* (2018).
- [6] Trafton Drew, Melissa L-H Vö, and Jeremy M Wolfe. 2013. The invisible gorilla strikes again: Sustained inattentive blindness in expert observers. *Psychological science* 24, 9 (2013), 1848–1853.
- [7] Lasse Hansen. 2019 (accessed 2020-04-22). *Tutorial: Abdominal CT Image Synthesis with Variational Autoencoders using PyTorch*. <https://medium.com/miccai-educational-initiative/tutorial-abdominal-ct-image-synthesis-with-variational-autoencoders-using-pytorch-933c29bb1c90>
- [8] Diederik P Kingma and Max Welling. 2014. Auto-encoding variational bayes. *International Conference on Learning Representations* (2014).
- [9] Michael Kistler, Serena Bonaretti, Marcel Pfahrer, Roman Niklaus, and Philippe Büchler. 2013. The virtual skeleton database: an open access repository for biomedical research and collaboration. *Journal of medical Internet research* 15, 11 (2013).
- [10] Geert Litjens, Thijs Kooi, Babak Ehteshami Bejnordi, Arnaud Arindra Adiyoso Setio, Francesco Ciompi, Mohsen Ghahfoorian, Jeroen A.W.M. van der Laak, Bram van Ginneken, and Clara I. Sánchez. 2017. A survey on deep learning in medical image analysis. *Medical Image Analysis* 42 (2017), 60 – 88.
- [11] Bjoern H Menze, Andras Jakab, Stefan Bauer, Jayashree Kalpathy-Cramer, Keyvan Farahani, Justin Kirby, Yuliya Burren, Nicole Porz, Johannes Slotboom, Roland Wiest, et al. 2014. The multimodal brain tumor image segmentation benchmark (BRATS). *IEEE transactions on medical imaging* 34, 10 (2014), 1993–2024.
- [12] Andriy Myronenko. 2018. 3D MRI brain tumor segmentation using autoencoder regularization. In *International MICCAI Brainlesion Workshop*. Springer, 311–320.
- [13] Danilo Jimenez Rezende, Shakir Mohamed, and Daan Wierstra. 2014. Stochastic Backpropagation and Approximate Inference in Deep Generative Models. In *Proceedings of the 31st International Conference on Machine Learning*. 1278–1286.
- [14] T Tashiro, T Matsubara, and K Uehara. 2017. Deep neural generative model for fMRI image based diagnosis of mental disorder. In *International Symposium on Nonlinear Theory and its Applications (NOLTA)*.
- [15] Nicholas J. Tustison, Brian B. Avants, Philip A. Cook, Yuanjie Zheng, Alexander Egan, Paul A. Yushkevich, and James C. Gee. 2010. N4ITK: Improved N3 Bias Correction. *IEEE Trans. Med. Imaging* 29, 6 (2010), 1310–1320.
- [16] David C Van Essen, Kamil Ugurbil, E Auerbach, D Barch, TEJ Behrens, R Buncholz, Acer Chang, Liyong Chen, Maurizio Corbetta, Sandra W Curtiss, et al. 2012. The Human Connectome Project: a data acquisition perspective. *Neuroimage* 62, 4 (2012), 2222–2231.
- [17] Ha Son Vu, Daisuke Ueta, Kiyoshi Hashimoto, Kazuki Maeno, Sugiri Pranata, and Sheng Mei Shen. 2019. Anomaly Detection with Adversarial Dual Autoencoders. *arXiv:1902.06924* (2019).
- [18] David Zimmerer, Simon AA Kohl, Jens Petersen, Fabian Isensee, and Klaus H Maier-Hein. 2019. Context-encoding Variational Autoencoder for Unsupervised Anomaly Detection. *Medical Imaging with Deep Learning (MIDL 2019)* (2019).
- [19] David Zimmerer, Jens Petersen, Simon AA Kohl, and Klaus H Maier-Hein. 2019. A Case for the Score: Identifying Image Anomalies using Variational Autoencoder Gradients. *arXiv preprint arXiv:1912.00003* (2019).

¹<https://ida.loni.usc.edu/login.jsp>

²<https://www.med.upenn.edu/sbia/brats2018/data.html>